



# Surface hydrophilic modification of PVDF membranes based on tannin and zwitterionic substance towards effective oil-in-water emulsion separation

Yongli Sun, Ying Zong, Na Yang, Na Zhang, Bin Jiang, Luhong Zhang\*, Xiaoming Xiao

School of Chemical Engineering and Technology, Tianjin University, Tianjin 300072, PR China

## ARTICLE INFO

### Keywords:

Tannin  
Zwitterion  
Superhydrophilicity  
Underwater superoleophobicity  
Oil-in-water emulsion separation

## ABSTRACT

Hydrophobic polyvinylidene fluoride (PVDF) membrane was successfully modified through a facile co-deposition strategy to improve its hydrophilicity and resistance to oil-fouling. The new zwitterion, sulfonated N, N-Diethylethylenediamine (DEDAPS), was synthesized via the ring-opening reaction and co-deposited with tannin acid (TA) on the surface of PVDF membranes. The obtained membranes were characterized by various techniques and utilized to separating oil-in-water emulsions. By controlling the concentration of DEDAPS in dipping solution, the pure water flux of the optimal membrane reached a maximum, which was 17 times that of the pristine membrane. In addition, the optimized membrane was endowed with superhydrophilicity and underwater superoleophobicity. It showed superb reusability and sustainability in separating various oil-in-water emulsions with the efficiency beyond 96%, which was attributed to the firm adhesion of co-deposition layer on the surface. This work might provide a new avenue for surface modification of membranes to be potentially used in oily wastewater purification.

## 1. Introduction

With the rapid development of industry and the acceleration of urbanization of human society, a tremendous amount of oil-contaminated waste water is increasingly produced by the emission of industrial process and oil spill catastrophe, bringing much menace to the sustainability of natural environment and the survival of creatures [1]. Conventional techniques for oil-polluted wastewater treatment such as gravity separation, adsorption, air floatation and centrifugation are usually low efficient or highly energy consumptive [2]. Additionally, these means are more useful to remediate oil/water mixture (oil diameter > 10  $\mu\text{m}$ ) rather than to deal with oil-in-water emulsions (0.1  $\mu\text{m}$  < oil diameter < 10  $\mu\text{m}$ ). Thus, it is crucial to develop facile and low-cost methods to overcome the disadvantages of traditional ways and to be well employed in separating oil-in-water emulsions [3]. Because of the unique superiorities such as no phase transformation, simple process, and low energy consumption, membrane separation technology based on the mechanism of wettability diversity and sieving effect has been considered as one of the most promising technologies in recent years, which can be employed in emulsions treatment with better performance [4] (see Scheme 1).

Polyvinylidene fluoride (PVDF), a typical polymeric membrane material with excellent physicochemical stability and strong

mechanical property, has been widely adopted in the field of micro-filtration (MF), ultrafiltration (UF), nanofiltration (NF), reverse osmosis (RO), gas separation, membrane bio-reactor, membrane distillation and fuel cells [5–12]. However, the intrinsic hydrophobicity of PVDF membranes makes them prone to be fouled in the filtration process, especially in separating oil-in-water emulsions, leading to the decrease of water flux and rejection [13,14]. It is known that being contamination shortens the service life of membranes and increases the application cost. To address these intractable issues, many scholars and researchers are devoted to exploring new ways to endow the membrane with hydrophilicity to improve its anti-fouling performance, which involve physical blending, surface segregation, surface grafting, surface coating, and surface bio-adhesion [15–22]. For instance, Jin's group fabricated a superhydrophilic and underwater superoleophobic PVDF membrane with a surface segregation approach and the as-prepared membrane exhibited good performance in treating oil-in-water emulsions [23]. Zhu and co-workers reported a kind of zwitterionic hydrogels grafted PVDF membrane, which showed superb antifouling property in dealing with oil-in-water emulsions containing complicated components [24]. Although these ways endowed the modified membranes with desirable separation effectiveness in the treatment of oil wastewater, they still have some shortcomings such as complex preparation process and the difficulty of scale-up in practical manufacture.

\* Corresponding author.

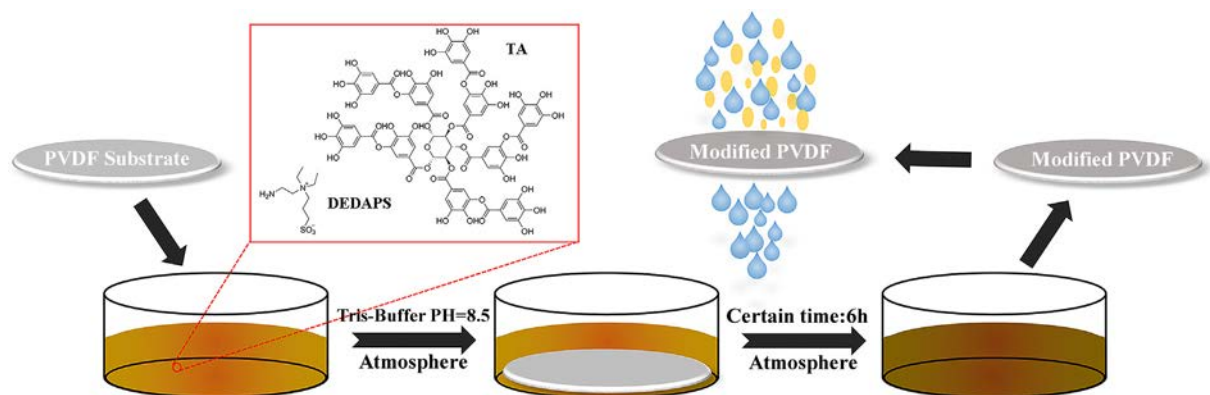
E-mail address: [zhanglvh@tju.edu.cn](mailto:zhanglvh@tju.edu.cn) (L. Zhang).

<https://doi.org/10.1016/j.seppur.2019.116015>

Received 12 June 2019; Received in revised form 1 September 2019; Accepted 1 September 2019

Available online 03 September 2019

1383-5866/ © 2019 Elsevier B.V. All rights reserved.



**Scheme 1.** Schematic illustration of the fabrication process of modified membrane and its application for emulsion separation.

In the methods mentioned above to improve the fouling resistance of membranes, surface bio-adhesion shows preponderance compared to others thanks to the simple dip-coating, decent stability and no post-processing. Since mussel-inspired catechol chemistry was first reported by Messersmith et al. in 2007, an increasing number of researchers have been concentrating on the hydrophilicity modification of membranes based on this manner [25]. For example, Shao et al. created superhydrophilic PVDF membranes by the crosslinking between poly-dopamine (PDA) and tetraethoxysilane and the obtained membranes exhibited good separation performance when disposing oil-in-water emulsions [26]. In the study of Qi et al., a superhydrophilic PVDF membrane with hierarchical surface structure was successfully developed to efficiently separate oil-in-water emulsions through two-step dip-coating of DPA and glutathione [22]. Nevertheless, the high cost of dopamine, the dark color as well as non-uniformity of PDA-involved coatings are unwished in practical application.

Fortunately, plant polyphenols such as epigallocatechin gallate (EGCG), gallic acid (GA), tannic acid (TA), epicatechin gallate (ECG) and pyrogallol (PG) recently have been reported as precursors in forming the light-colored multifunctional coatings on the surface of various solid materials [27,28]. Among them, TA, widely distributed in plant tissues, attracted our great attention in the context of surface bioadhesion modification due to its cheap price and easy storage. TA can strongly adhere to substrate surface via constructing covalent and non-covalent bonding structures after the oxidation of catechol moiety into quinone under weak alkaline condition [27–30]. In addition, TA can form a composite coating on the membrane surface with other substances because of the quinone moiety. Researches about TA co-depositing with chemicals such as metal ions, silane coupling agents and polymers via forming coordination network, nanostructures and crosslinking structures, respectively, have been reported. For instance, Zhu et al. prepared a superhydrophilic membrane by forming  $\text{Fe}^{3+}$ -polyphenol coordination network on its surface with the co-deposition of TA and ferric ions [31]. Li's group employed the one-step co-deposition of TA and 3-aminopropyltriethoxysilane (APTES) to construct hierarchical nanospheres on the membrane surface through Michael addition and Schiff's base reactions [21]. And furthermore, another coating was formed on the TA/APTES layer via the co-deposition of TA and polyethyleneimine (PEI), resulting in multiple hierarchical structures [32]. These superhydrophilic modified membranes based on TA were efficient in treating the oil-in-water emulsions. Besides the aforementioned agents co-deposited with TA, zwitterions are another category of attractive fouling resistances, which have also been widely used in membrane modification. Due to the attraction force between the positive/negative charges and water molecules, zwitterion can robustly confine water molecules around the zwitterionic groups and form a compact hydration shell to repel the contaminant [33]. The methods of employing the zwitterion materials in membrane modifications mainly involve surface grafting, interfacial polymerization

and blending strategy. For example, Xue's group reported a poly(lactic acid) hemodiafiltration membrane with enhanced fouling resistance and hemocompatibility by grafting zwitterionic poly(sulfobetaine methacrylate) (PSBMA) on membrane surfaces [34]. Jiang et al. prepared a novel nanofiltration membrane to be employed in dye and inorganic salt removal by interfacial polymerization of a novel zwitterionic amine monomer PEI-g-SBMA and Trimesoyl chloride (TMC) [35]. Papatya and co-workers synthesized two zwitterionic copolymers based on methyl methacrylate (MMA) to be used as surface segregating additives to prepare modified PVDF membrane, which showed better performance than the additive-free PVDF membrane [36]. However, seldom researches have been reported about TA depositing with micromolecular zwitterionic substance on membrane surfaces for separating oil-in-water emulsions.

Herein, we synthesized a micromolecular zwitterion (DEDAPS) with an amino moiety through the open-ring reaction and the new substance was successfully applied to be co-deposited with TA on PVDF membrane via Michael addition reaction and Schiff's base reaction under weak alkaline condition. The structure of zwitterion was verified by means of FTIR, NMR and Mass spectrometry. The underlying mechanism of co-deposition was investigated on basis of UV-vis and XPS analysis. The influences of TA concentration, pH value of feed, surfactant types on membrane performance were investigated. And the impacts of different concentration of zwitterion in co-deposition aqueous solution towards chemical constitution, surface morphology, and performance of the as-prepared membranes were explored in detail. Moreover, the coating stability, cyclic reusability and long-term stability were also tested to evaluate the sustainability of the membranes. The superhydrophilic and underwater superoleophobic PVDF membrane fabricated by the co-deposition of TA and DEDAPS might have the potential practical application in oil-in-water emulsion purifications.

## 2. Experimental section

### 2.1. Materials

Commercial PVDF microfiltration membranes (MF, the size diameter of 10 cm, average pore diameter of 0.1  $\mu\text{m}$ ) were purchased from Zhongli Filtration Equipment Factory (China). N, N-Diethylethylenediamine (DEDA, 98%), Tannin Acid (TA, AR) and Carbon tetrachloride ( $\text{CCl}_4$ , IR) were obtained from Kermel (Tianjin) chemical reagents Co., Ltd. (China). 1, 3-Propanesultone (1, 3-PS, 99%) was bought from Dibo (Shanghai) chemical Technology Co., Ltd. (China). Ethyl acetate (AR), ethanol (EtOH, AR) and Sodium dodecyl sulphate (SDS, AR) were supplied by Yuanli Chemical Technology Co., Ltd. (Tianjin, China). Tween 80 (AR) and Hexadecyl trimethyl ammonium Bromide (CTAB, AR) were purchased from Tianjin fine chemical research institute (China). Tris (hydroxymethyl)-aminomethane (Tris-

HCl, pH = 8.5) was obtained from Senbeijia (Nanjing) biological technology Co., Ltd. (China). Deionized water was used in all experiments. All chemicals were used as received without further purification.

## 2.2. Preparation of modified PVDF membrane

### 2.2.1. Synthesis of new zwitterionic substance-DEDAPS

Sulfonated N, N-Diethylethylenediamine (DEDAPS) was synthesized by the ring opening reaction of 1, 3-PS and DEDA. Firstly, DEDA (7.55 g) and ethyl acetate (80 mL) were put into a 250 mL round bottom flask equipped with a stirrer at 30 °C. Then a solution of 10 mL ethyl acetate containing 7.33 g 1, 3-PS was added to the stirred solution dropwise for 60 min. After reaction for 5 h at 30 °C, the liquid reaction system turned from transparent solution to milky white suspension. The white crude product was collected by filtration and eluted completely with ethyl acetate to remove unreacted reagents. Finally, the white product was dried under vacuum at 80 °C for 24 h to a constant weight.

### 2.2.2. Preparation of composite PVDF membranes

For starters, pristine PVDF membranes were immersed in ethanol for 60 min to clean surfaces and pores of membranes, and then soaked in deionized water for another 60 min to wash away the ethanol, the pre-treated membranes above were labeled as M0. Next, M0 was soaked in deionized water for 6 h, which was called M-Pristine after complete drying in the air drying oven at 50 °C. Then, a certain amount of DEDAPS and 0.5 g of TA were dissolved in 100 mL of Tris-HCl solution (pH = 8.5) and M0 was immersed in the buffer solution at room temperature for 6 h under mild agitation on a rocking platform, the obtained membrane of which was noted as M-TA5#X, where X presented the concentration of DEDAPS in buffer solution. The concentration of TA was optimized previously and determined at 5 g/L (Fig. S1). As a control, PVDF membrane modified with TA in the absence of DEDAPS under the same conditions was also fabricated, which was labeled as M-TA5#0.

## 2.3. Characterization

The NMR of DEDAPS was analyzed using NMR spectrometer (VARIAN INOVA 500 MHz, VARIAN, USA). The mass spectrum of DEDAPS was detected by mass spectrometer (Bruker, solanX 79 FT-MS, Germany). The ultraviolet-visible (UV-vis) absorption of co-deposition solution was measured with UV-vis spectrophotometer (UV-4802S, Unico, USA). The porosity and pore size distribution of membranes were measured by porosity analyzer (3H-2000 TD2, Beishide, China) and pore size analyzer (3H-2000 PB, Beishide, China), respectively. The chemical structures of membranes and DEDAPS were analyzed by attenuated total reflectance Fourier transform infrared spectroscopy (ATR-FTIR, Bruker, TENSOR II, Germany) and Elements composition was characterized by X-ray photoelectron spectra (XPS, Thermo ESCALAB 250Xi, USA). The surface morphologies were characterized by scanning electron microscopy (SEM, Hitachi, S-4800, Japan) and the surface roughness of membranes was determined by atomic force microscopy (AFM, multimode 8, Bruker, Germany) in the tapping mode. The thermal analysis was evaluated by Differential Scanning Calorimeter (DSC) (METTLER TOLEDO DSC1, METTLER TOLEDO, Switzerland). Surface charges were determined by a surpass electrokinetic analyzer (Surpass, Anton Paar, Austria). The water contact angle (WCA) and underwater oil contact angle (UOCA) were measured with JC 2000 goniometer (Powereach, China) by directly dropping liquid droplet on the surface of the membrane. Oil droplet size distribution was detected by a dynamic light scattering (DLS) particle size analyzer (Nano ZS, Malvern, UK).

## 2.4. Filtration and antifouling performance test

All oil/water emulsions separation experiments were carried out at

1 bar using a self-made dead-end stirred filtration cell. The effective filtration area of tested PVDF membranes is 33.18 cm<sup>2</sup>. Five kinds of selected oil, including diesel, n-hexane, kerosene petroleum ether and dichloromethane, were used as sample oils for emulsions separation tests. With sodium dodecyl sulfate (SDS) as emulsifier, the surfactant-stabilized oil-in-water emulsions were prepared by stirring the mixture of oil and water (g/g = 1:1000) using a homogenizer (Fluke homogenizer, FA25, 500 W) operated at 19,000 rpm for 30 min. For each separation experiment, a certain volume of oil-in-water emulsion was poured into the solution reservoir after the placement of PVDF membrane on the bottom and then the filtration solution was collected for calculating the permeation and separation efficiency. Every reusability test was conducted for 6 cycles and a water rinsing treatment was implemented to recover the filtration performance of measured membranes. Both the micrographs of feed solution and filtration solution were captured using an optical microscope. The values of the oil contents were obtained from the means of five measurements per sample. The flux (J), rejection (R) and flux recovery ratio (FRR) were calculated using the following equations:

$$J = \frac{V}{A\Delta t} \quad (1)$$

where V, A and Δt corresponds to the volume of feed solution (L), the separation membrane area (m<sup>2</sup>) and the filtration time (h), respectively.

$$R (\%) = \left(1 - \frac{C_2}{C_1}\right) \times 100\% \quad (2)$$

where C<sub>1</sub> (mg/L) refers to the oil concentration of the feed and C<sub>2</sub> (mg/L) is the oil concentration of the filtrate, which was measured with an infrared oil content analyzer (F2000, China) after being extracted by CCl<sub>4</sub>.

$$FRR(\%) = \frac{J_2}{J_1} \times 100\% \quad (3)$$

where J<sub>1</sub> (L·m<sup>-2</sup>·h<sup>-1</sup>) is the first pure water flux and J<sub>2</sub> (L·m<sup>-2</sup>·h<sup>-1</sup>) is the pure water flux after filtration.

## 2.5. Long-term stability test of the membranes

In view of the significance of modified membranes in long-term separation behavior, the novel membranes are supposed to possess the robust stability in separation tests. For verifying the long term steadiness of modified PVDF membranes, diesel-in-water emulsion was chosen as representative sample to evaluate the persistent separation performance including emulsion flux, oil rejection and flux recovery ratio. The test was conducted once a day and last two weeks. The surface morphology and UOCA of the membrane were evaluated before and after long-term tests.

## 3. Results and discussion

### 3.1. The chemical analyses and the underlying mechanism of TA/DEDAPS co-deposition

Fig. 1a showed the ring-opening reaction of DEDA and 1, 3-PS and the chemical structure of DEDA and DEDAPS were investigated by <sup>1</sup>H NMR (Fig. 1b). Compared with the spectrum of DEDA, several new peaks appeared in the spectrum of DEDAPS, which were labeled as a, b, c, d, e, f and g, respectively. In detail, protons a (δ = 3.19 ppm), b (δ = 3.11 ppm), c (δ = 3.02 ppm) and e (δ = 2.72 ppm) were held by carbon atoms in α-position of the quaternary ammonium ion of DEDAPS, while protons d (δ = 2.94 ppm) and f (δ = 2.25 ppm) were carried by those in α- and β-positions of the sulfonate group [37]. The discussions about <sup>13</sup>C NMR (Fig. S2) and mass spectrum (Fig. S3) of DEDAPS were presented in the [supplementary materials](#). These analyses proved that the DEDAPS had been successfully synthesized.

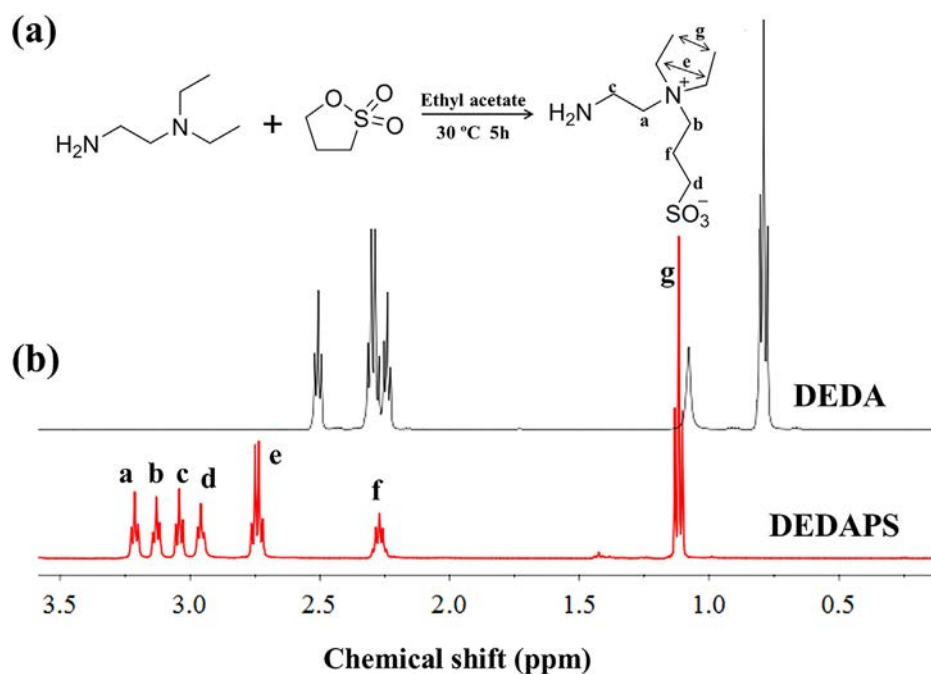


Fig. 1. (a) The reaction of DEDA and 1, 3-PS and (b)  $^1\text{H}$  NMR spectra of DEDA and DEDAPS.

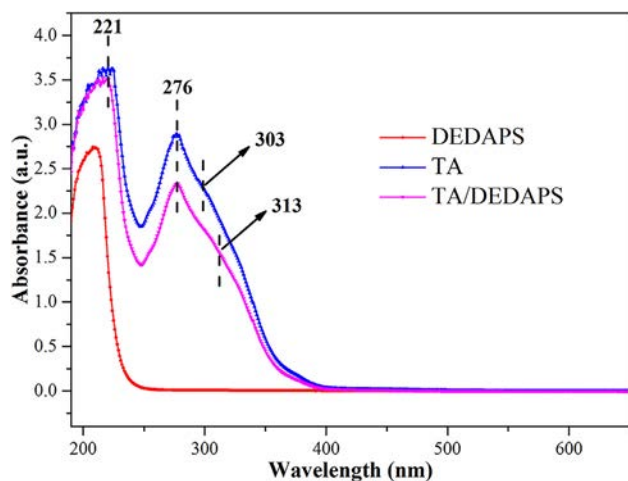


Fig. 2. UV-vis spectra of different aqueous solutions.

The possible chemical reactions and interactions between TA and DEDAPS can be speculated from UV-vis spectra of different solutions after centrifugation. Fig. 2 exhibited that the absorbance of solution only containing TA showed a peak at 221 nm and a slightly broadened peak at 276 nm, which were attributed to the inherent neutral form of TA. And the peak at 303 nm was due to the phenolate form of TA [38]. However, when DEDAPS was added, the broad peak shifted to longer wavelengths at 313 nm while there was no visible peak around 313 nm in the absorbance of DEDAPS solution, which could be explained by the possible reactions and non-covalent interactions between TA and the zwitterion. The DSC and  $^1\text{H}$  NMR spectra were provided in supplementary materials to explore the possible interactions between TA and DEDAPS. As a result, the heat release of M-TA5#3 was higher than that of the others (Fig. S4) and the obvious changes of chemical shifts were observed in the  $^1\text{H}$  NMR spectrum in Fig. S5.

FTIR analysis was utilized to investigate the surface chemistry of pristine membrane and modified membranes and the structure of DEDAPS. As shown in Fig. 3, the characteristic strong absorption peaks at 1403 and 1180  $\text{cm}^{-1}$  were ascribed to the stretching vibration of

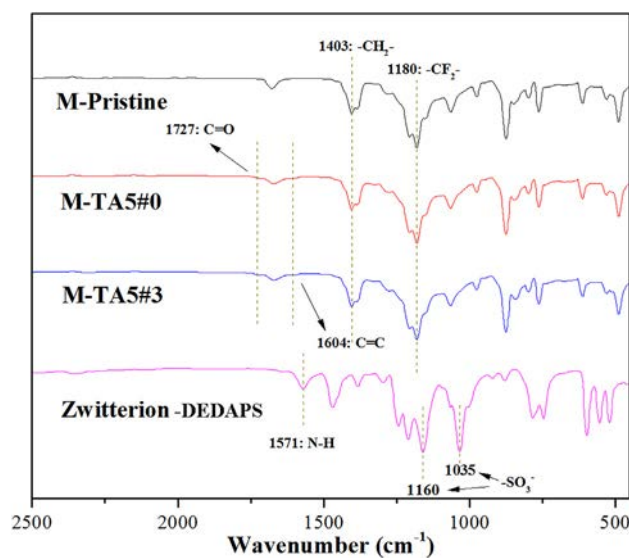


Fig. 3. FTIR spectra of prepared membranes and the zwitterion.

$-\text{CH}_2$  and  $-\text{CF}_2$  in PVDF substrate [39]. Compared with the pristine PVDF membrane, M-TA5#0 and M-TA5#3 both exhibited two new peaks at 1727 and 1604  $\text{cm}^{-1}$ , which were assigned to stretching vibration of  $\text{C}=\text{O}$  and  $\text{C}=\text{C}$ , respectively, indicating that TA had undergone self-oxidation and been deposited on the surface of membranes [40]. The peaks at 1571, 1160 and 1035  $\text{cm}^{-1}$  represented the  $\text{N}-\text{H}$  bending vibration,  $\text{S}=\text{O}$  asymmetric stretching and  $\text{S}=\text{O}$  symmetric stretching, further confirming the synthesis of DEDAPS [41]. However, these peaks could not be observed obviously on the spectrum of M-TA5#3. The reason might be that the amount of DEDAPS on membrane surface was limited and the peaks could be covered by the intrinsic strong peaks of the pristine PVDF membrane.

To further gain more information about the chemical constitution of as-prepared membranes, XPS was employed to analyze the elements on the surface. As listed in Table 1, M-Pristine mainly consisted of 51.80% carbon and 48.09% fluorine, while for M-TA5#0, the carbon content increased to 55.90%, and the fluorine content decreased to 36.94%,

**Table 1**  
Elemental composition of different PVDF membranes.

Membrane	Composition (%)				
	C	N	O	F	S
M-Pristine	51.80	0	0.11	48.09	0
M-TA5#0	55.90	0	7.16	36.94	0
M-TA5#3	54.47	2.57	7.24	34.57	1.15

which was ascribed to the individual-deposition of TA. Compared with M-TA5#0, M-TA5#3 had extra 2.57% nitrogen and 1.15% sulfur, manifesting that TA and DEDAPS co-deposited on the surface of membranes. And the ratio of N/S was close to 2:1, which was consistent with the corresponding atom proportions in DEDAPS. In general, TA had two intrinsic peaks at 533.5 eV and 529.4 eV in the O 1s, attributing to the C=O and HO-C groups, respectively. [42] However, the peak of HO-C group spectrum shifted from 529.4 eV to a higher binding energy of 531.8 eV (Fig. 4b) after co-deposition, which was due to electrons transfer of TA caused by the non-covalent interaction between TA and DEDAPS [42]. Furthermore, it could be seen from Fig. 4c that three nitrogen species were located at 399.4 eV, 400.4 eV, and 401.7 eV, which were assigned to the C-N of the amide, C=N of amide and  $N^+-(CH_2)_4$  of quaternary ammonium ion, respectively [43]. The peak of C-N belonged to the DEDAPS or the bond generated by Michael addition reaction between TA and the zwitterion. The new peak of C=N suggested the self-oxidized TA reacted with DEDAPS Schiff's base reaction and then deposited on the membrane surface together. The peak occurring at 401.7 eV belonged to the  $N^+-(CH_2)_4$  group of DEDAPS, confirming that the tertiary amine moiety of DEDA turned into quaternary ammonium ion by reacting with 1, 3-PS. Besides, the

appearance of  $-SO_3^-$  at 168.1 eV (Fig. 4d) further confirmed the co-deposition of TA and DEDAPS [44]. In brief, these XPS analyses verified that TA and DEDAPS successfully deposited on pristine PVDF membrane surfaces together.

On the basis of the characterization analyses above, the possible mechanism was put forward for the co-deposition process. As shown in Scheme 2a, TA with five trihydroxyphenyl moieties underwent the initial self-oxidation and then the formed quinone structure further reacted with DEDAPS via Michael addition reaction and Schiff's base reaction. In the matter of the former reaction (Michael addition), it generally happened between the amino group (electron donor) and the benzoquinone structure (electron acceptor). As for Schiff's base reaction, it referred to the condensation reaction occurred between the amine and active carbonyl group. Specifically, amino group attacks the carbonyl of quinone generated from the oxidation of catechol moiety of TA [5]. Besides covalent bonds of TA and DEDAPS, the electrostatic attractions between quaternary ammonium ion and sulfonic group as well as hydrogen bonds also contributed to the formation of coating on membrane surface (Scheme 2b).

### 3.2. Surface properties of the as-prepared membranes

Surface morphology variations were characterized by SEM and AFM. As depicted in Fig. 5a and b, it was porous on the surface of M-Pristine obviously. Fig. 5c and d showed that the TA coating formed on the surface of M-TA5#0, and micropores of the membrane were partially covered by the coating. Interestingly, after co-deposition of TA and DEDAPS, the surface of M-TA5#3 (Fig. 5e and f) arose a denser structure, which was caused by the multifarious-actions including chemical covalent bonds, electrostatic interactions and hydrogen bonds when forming the composite coating. There were slight changes in the

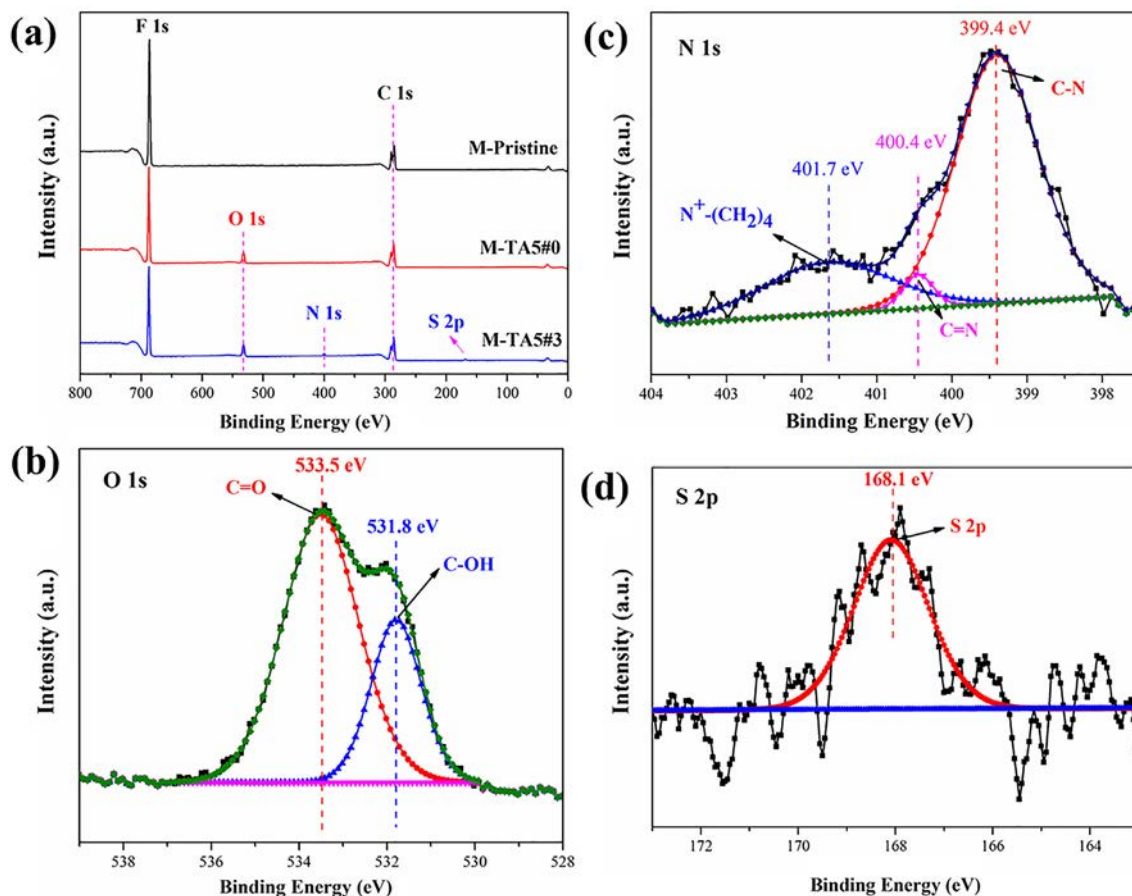
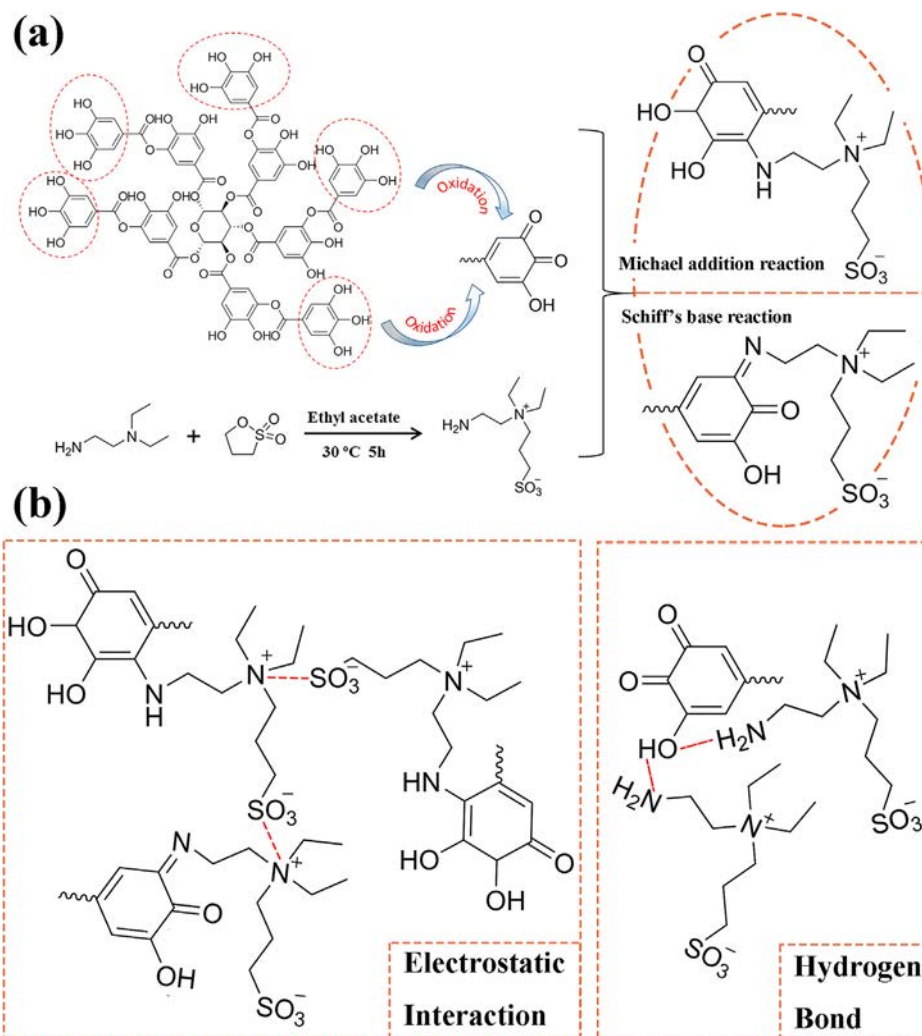


**Fig. 4.** (a) XPS spectra of M-Pristine, M-TA5#0 and M-TA5#3 and (b–d) are the high-resolution XPS analysis of O 1s, N 1s and S 2p of M-TA5#3 respectively.



**Scheme 2.** The possible mechanism for the TA/DEDAPS co-deposition process including (a) covalent bonds and (b) non-covalent bonds.

porosity and pore size distribution of the base membrane and modified membranes (Fig. S6), demonstrating that the co-deposition strategy almost had no influence on the pore size distribution and porosity of membranes. As exhibited in three-dimensional AFM images, the average roughness (Ra) of M-TA5#0 was 76.1 nm while it was 92.5 nm of M-Pristine. The decrease of Ra could be explained by that the hydrophilic coating formed by TA covered a part of pores on membrane surfaces. However, compared with M-TA5#0, the Ra of M-TA5#3 increased to 124.6 nm. The rougher surface could be attributed to that the zwitterion in the co-deposition solution accelerated the deposition process of TA and co-deposited with TA as well. It also has been widely reported that the surface roughness contributed much to the wettability of membranes [45–47].

The cross-sectional SEM images of membranes were provided in Fig. 6. It can be seen from Fig. 6a that the cross-section of the commercial membrane was a sandwich structure and the middle layer was the nonwoven support layer. As shown in Fig. 6b–d, there appeared a coating on the original PVDF membrane and coating of M-TA5#3 was denser than that of M-TA5#0, which was consistent with the AFM analyses.

In addition, to evaluate the co-deposition layer stability of M-TA5#3, the rinsing and bending tests were conducted. As shown in Fig. S7, the coating was wrapped on the surface of membrane after vigorous rinsing and bending tests, and the underwater superoleophobicity was well reserved as well. The SEM images and UOCA of the membrane were also provided after immersing in various oils to further confirm

coating stability (Fig. S8). No obvious changes in morphology and surface wettability after stability tests demonstrated the good stability of the coating. The surface charges changes of the membranes were also tested (Fig. S9). The surface of M-TA5#3 was more negatively charged than that of the other two membranes, which was beneficial to pollutant removal and long-term use when separating emulsions stabilized by anionic surfactants [40].

### 3.3. The wettability of as-prepared membranes

Water contact angle (WCA) was the vital parameter to reflect the wettability of membranes, which influenced pure water flux (PWF) to a great extent. Fig. 7a showed the PWF of a series of membranes fabricated with different content of DEDAPS in co-deposition solution. Obviously, PWF of membranes increased significantly after modification of TA and DEDAPS. Specifically, PWF increased from  $277.3 \pm 20.9$  L/( $\text{m}^2\cdot\text{h}$ ) (M-Pristine) to  $3906.1 \pm 290.3$  L/( $\text{m}^2\cdot\text{h}$ ) (M-TA5#0) and to  $4701.6 \pm 385.2$  L/( $\text{m}^2\cdot\text{h}$ ) (M-TA5#3). The first improvement in PWF can be ascribed to hydrophilic groups of TA, which can form a hydration layer via forming hydrogen bond with water molecules. And the addition of DEDAPS in co-deposition solution led to further increase in PWF because the zwitterion can construct thicker hydration shell than hydrophilic groups through attracting more water molecules on the surface of membranes [15]. Moreover, PWF reached a plateau at  $4701.6 \pm 385.2$  L/( $\text{m}^2\cdot\text{h}$ ) and showed no changes with the further increase of DEDAPS concentration, which revealed that DEDAPS can

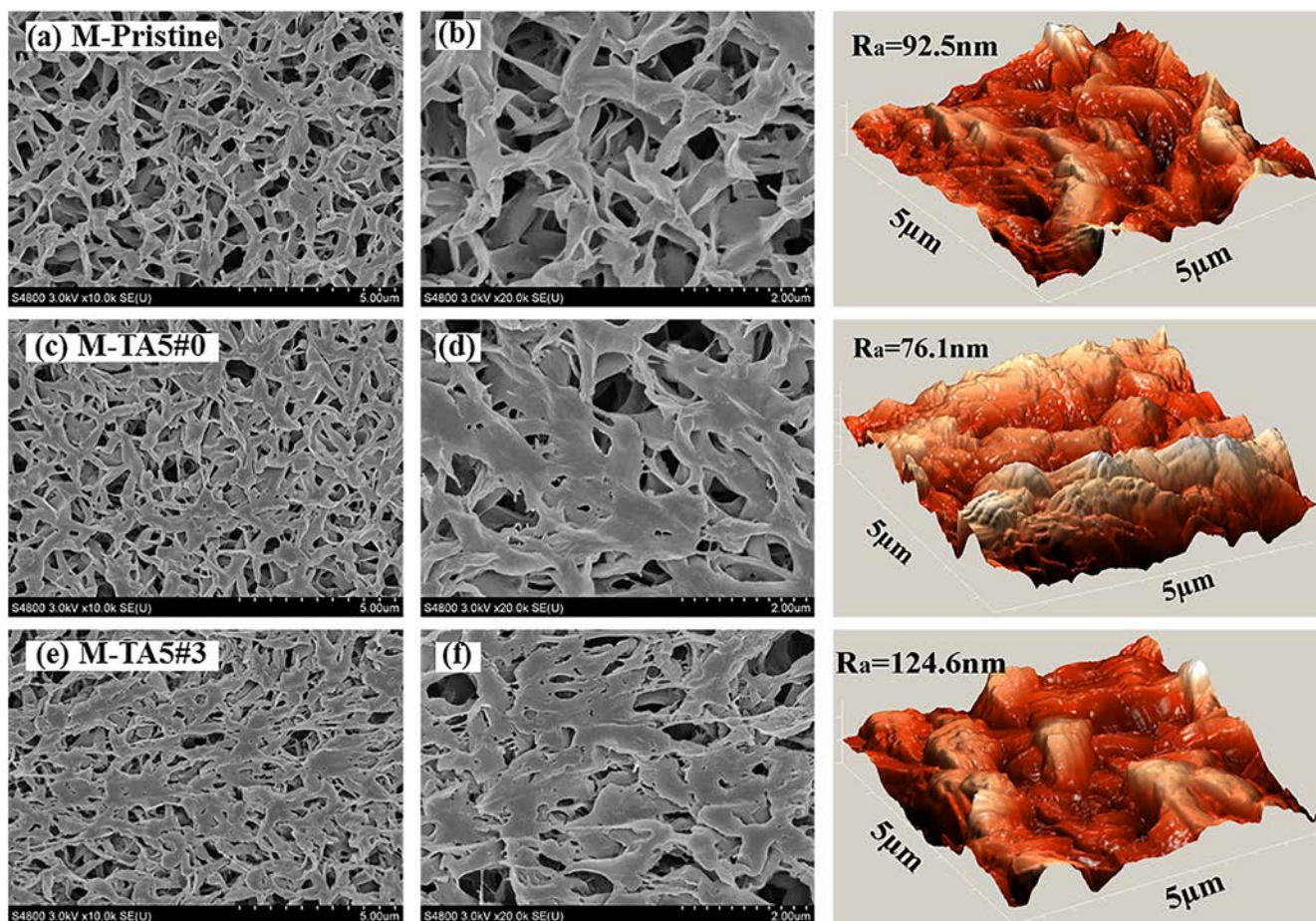


Fig. 5. SEM images (10 k × and 20 k ×) of surface morphology of (a, b) M-Pristine, (c, d) M-TA5#0 and (e, f) M-TA5#3, and the right figure is the corresponding AFM image.

deposit on the membrane surface with the assist of natural polyphenol TA and that there existed a co-deposition balance between the micro-molecular zwitterion substance and TA due to the limited bonding sites of TA. The relative weight gain was measured to verify this speculation. As shown in Fig. S10, the relative weight gains of the membranes

increased at first with the increase of DEDAPS concentration, and then it reached a maximum at  $1.05 \pm 0.08$  and kept unchanged as the further increasing of DEDAPS concentration.

It can be seen from Fig. 7b that the unmodified membrane exhibited hydrophobicity with the stabilized WCA of  $113^\circ$ . After the individual

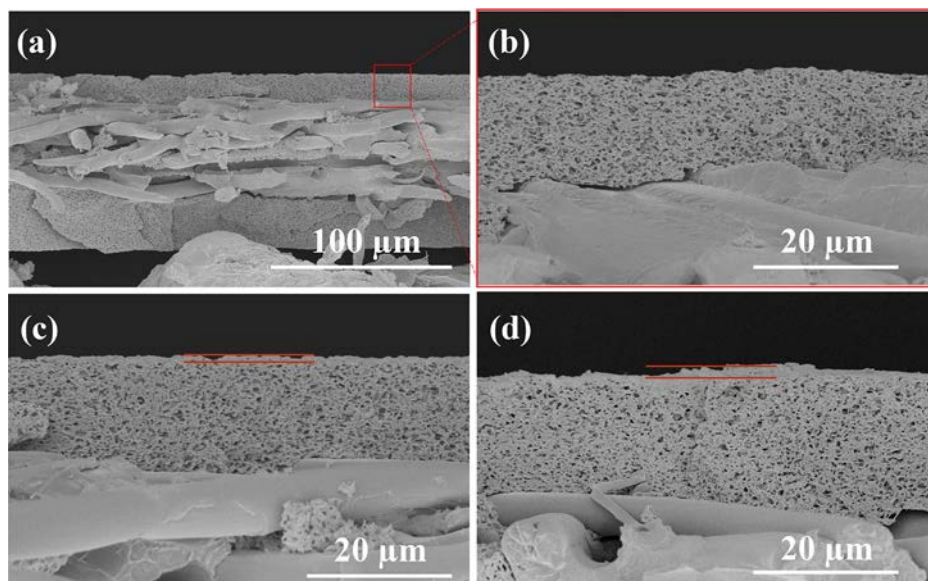


Fig. 6. Cross-sectional images of (a and b) M-Pristine, (c) M-TA5#0 and (d) M-TA5#3.

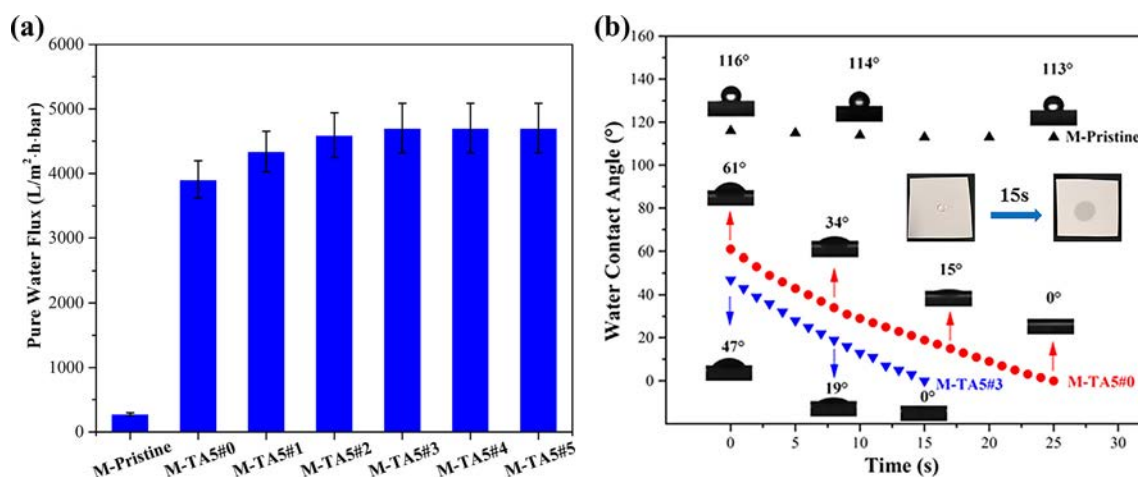


Fig. 7. (a) Pure water flux of the as-prepared membranes and (b) water contact angles of chosen membranes.

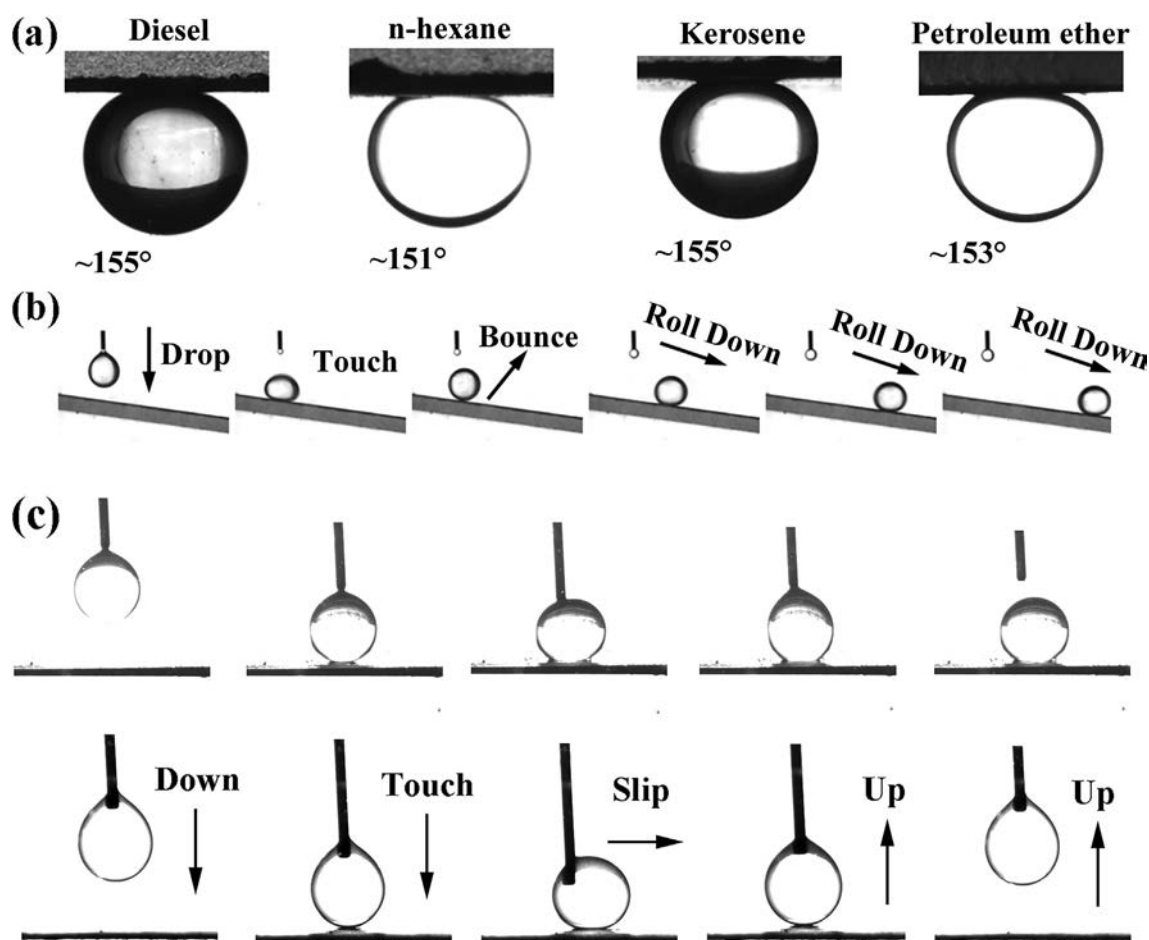


Fig. 8. (a) Under water oil contact angle of diesel, n-hexane, kerosene and petroleum ether, respectively, (b) the rolling contact test of dichloromethane on M-TA5#3 and (c) underwater oil-adhesion test of M-TA5#0 (upper) and M-TA5#3 (bottom).

deposition of TA, WCA of M-TA5#0 declined from 61° to 0° within 25 s, manifesting the improvement of membrane hydrophilicity. Furthermore, after the co-deposition of TA and DEDAPS, WCA of M-TA5#3 declined from 47° to 0° within 15 s, which indicated that the modified membrane was provided with more admirable hydrophilicity whether in the term of original water contact angle or the wetting time compared with M-TA5#0. The more hydrophilic surface of M-TA5#3 was endowed by the facial composite coating formed by TA and DEDAPS, which could trap more water molecules on the surface to form

hydration layer through hydrogen bonds due to the hydrophilic groups and zwitterions. The results demonstrated that the co-deposition strategy changed the membrane from hydrophobicity to superhydrophilicity.

Fig. 8a showed the underwater superoleophobicity of M-TA5#3, of which the underwater oil contact angle of diesel, n-hexane, kerosene and petroleum ether were about 155°, 151°, 155°, and 153°, respectively. A droplet of dichloromethane dropped on the surface of membrane with a tilt angle less than 7°. Then it underwent touching and

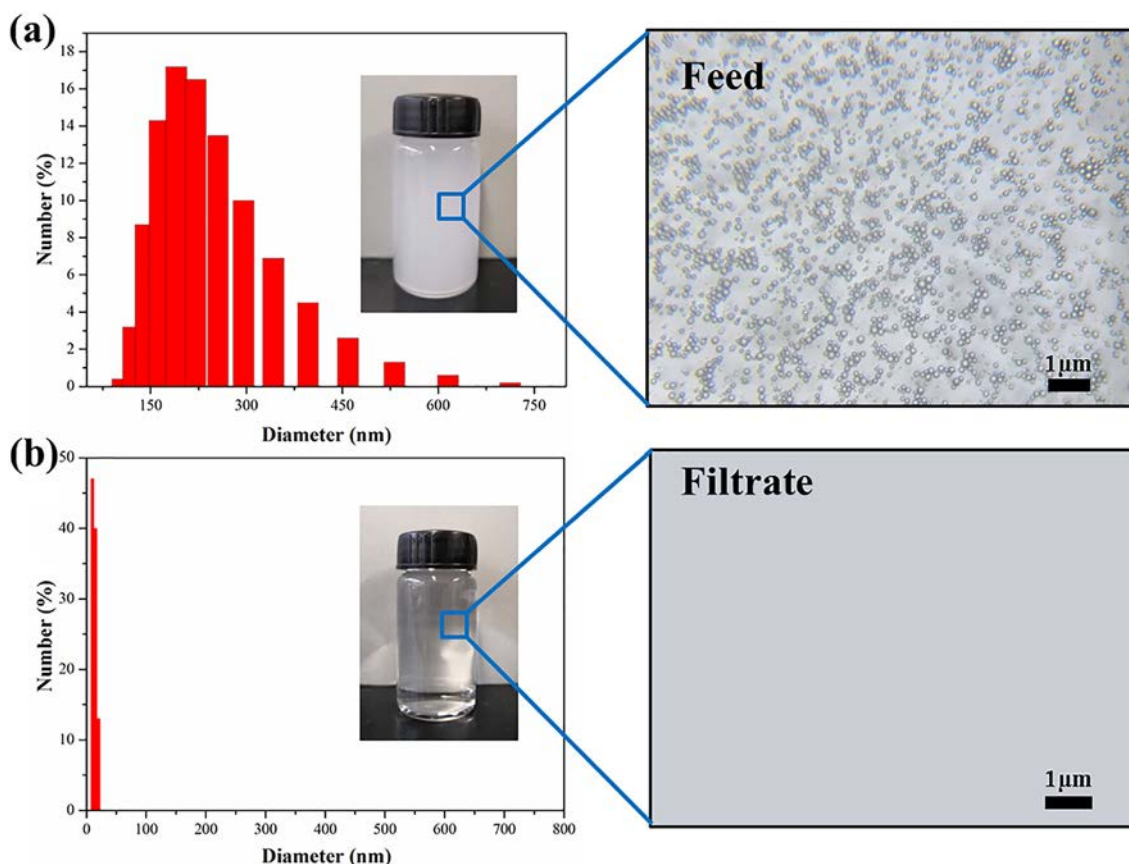


Fig. 9. Droplet size distributions of diesel-in-water emulsion determined by dynamic light scattering and micrographs analyses (a) before and (b) after filtration.

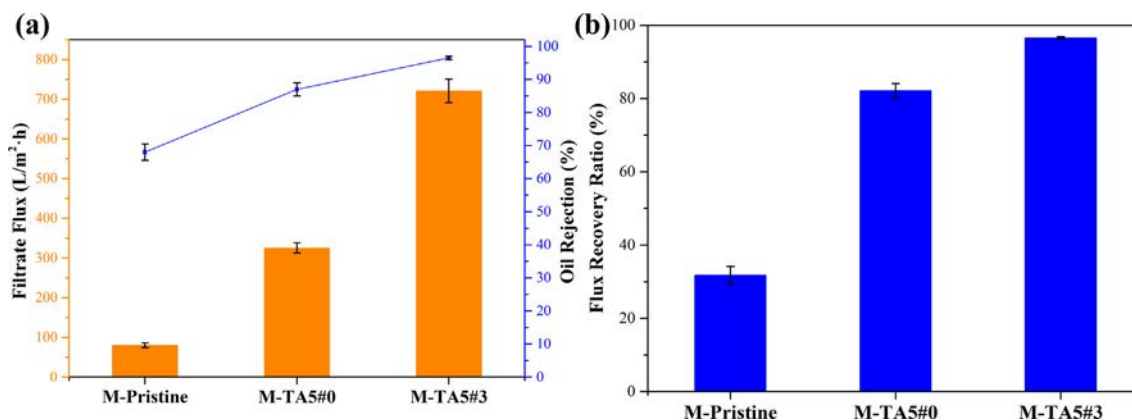


Fig. 10. Comparison of the (a) separation performance and (b) antifouling property among substrate membrane and modified membranes towards diesel-in-water emulsion.

bounce, and rolled down the as-fabricated membrane fast in the end (Fig. 8b). As demonstrated in Fig. 8c, the oil drop slipped away when pressed and then left the surface of M-TA5#3 along with needle easily while it stayed on M-TA5#0 surface, indicating the better underwater oleophobicity of M-TA5#3. This co-deposition membrane also maintained benign underwater oleophobicity with the pH of feed ranged from 4 to 12 (Fig. S11). It can be concluded that the superhydrophilic M-TA5#3 possessed ultralow oil adhesion, which could effectively protect the membrane from oil-fouling.

### 3.4. Oil-in-water emulsion separation performance of membranes

The co-deposition layer endowed PVDF membranes with superhydrophilicity and underwater superoleophobicity and might

simultaneously allow for benign emulsions separation property. Oil drop size distributions of diesel-in-water emulsion and filtrate were measured by the DLS analysis and optical microscope. Fig. 9a and b showed that the emulsion droplet size ranged from 100 nm to 600 nm before separation process and changed to almost 0 after filtration. In addition, it can be seen from micrographs that there were numerous nanoscale oil droplets in the feed while invisible in the filtrate. Obviously, the milky emulsion transformed to a transparent one after the treatment of the optimal membrane, M-TA5#3. The results indicated that the obtained membrane had high separation efficiency in tackling emulsions with nanoscale oil droplets.

The performance of M-Pristine and M-TA5#0 toward diesel-in-water emulsions stabilized by SDS were compared with M-TA5#3. As shown in Fig. 10a, M-TA5#3 possessed higher filtrate flux and oil

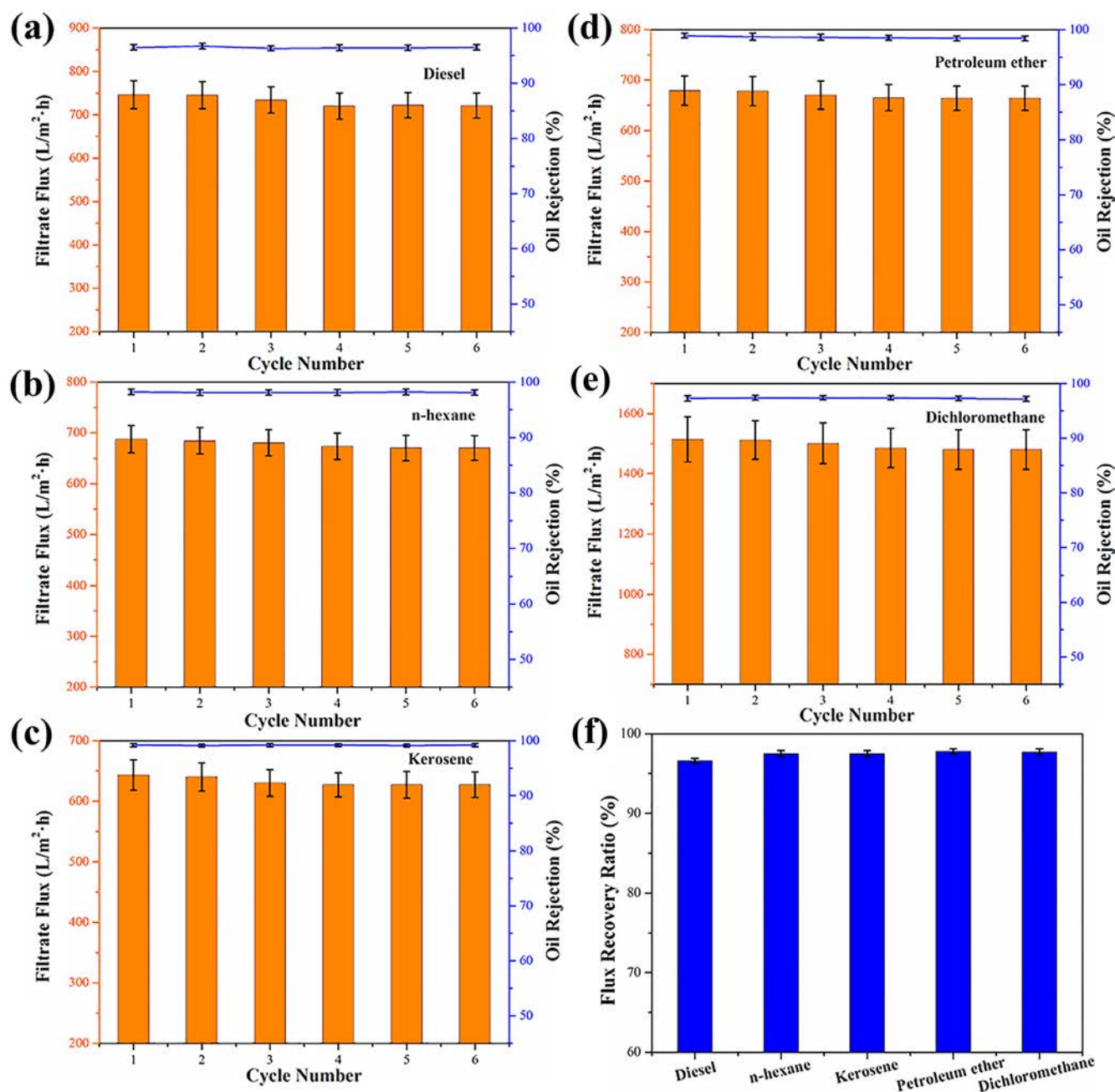


Fig. 11. The cycle tests of SDS emulsified oil-in-water emulsions of diesel, n-hexane, kerosene, petroleum ether and dichloromethane (a-e), respectively, and (f) flux recovery ratio of diverse emulsions.

Table 2

Comparison of performance of surface modified membranes for emulsions separation between literatures and this work.

Preparation Condition	WCA (°)	PWF (L/m <sup>2</sup> ·h)	Oil rejection	Literature
DPA/PEG-NH <sub>2</sub>	31 ± 4	4800 (0.03 MPa)	95.8%	[49]
DPA/GO	43.8 ± 2.2	/	96%	[50]
DPA/PEI	55	6200 (0.12 MPa)	/	[51]
TA/PEI	16	10,782 (0.1 MPa)	/	[3]
TA/DEDAPS	0	4701 (0.1 MPa)	> 96%	This work

rejection than the other two membranes. In detail, the filtrate flux of M-Pristine was only  $80.4 \pm 5.8$  L/m<sup>2</sup>·h, which was much lower than those of M-TA5#3 ( $721.2 \pm 29.7$  L/m<sup>2</sup>·h) and M-TA5#0 ( $325.7 \pm 12.7$  L/

m<sup>2</sup>·h). The low flux of M-Pristine could be attributed to its inherent hydrophobicity, which caused severely fouling and pore blockage of the membrane by oil droplets as the separation test proceeding. The filtrate flux of M-TA5#3 was higher than that of M-TA5#0 attributed to its better hydrophilicity and oleophobicity of M-TA5#3. The oil rejection of M-Pristine, M-TA5#0 and M-TA5#3 was  $68.1 \pm 2.5\%$ ,  $87.2 \pm 2.3\%$  and  $96.5 \pm 0.5\%$ , respectively. As the membranes possessed similar pore size distribution (Fig. S6), the difference in oil rejection could be explained by the different wettability of these membranes. As exhibited in Fig. 10b, the FRR of the original PVDF membrane was  $31.8 \pm 2.4\%$ , which could be explained by that the PVDF substrate was hydrophobic and easy to be fouled by oil. And the FRR of M-TA5#3 was higher ( $96.6 \pm 0.3\%$ ) than that of M-TA5#0 ( $82.1 \pm 2.0\%$ ), which was due to the better hydrophilic surface of M-TA5#3. In a word, M-TA5#3 possessed the best separation and anti-

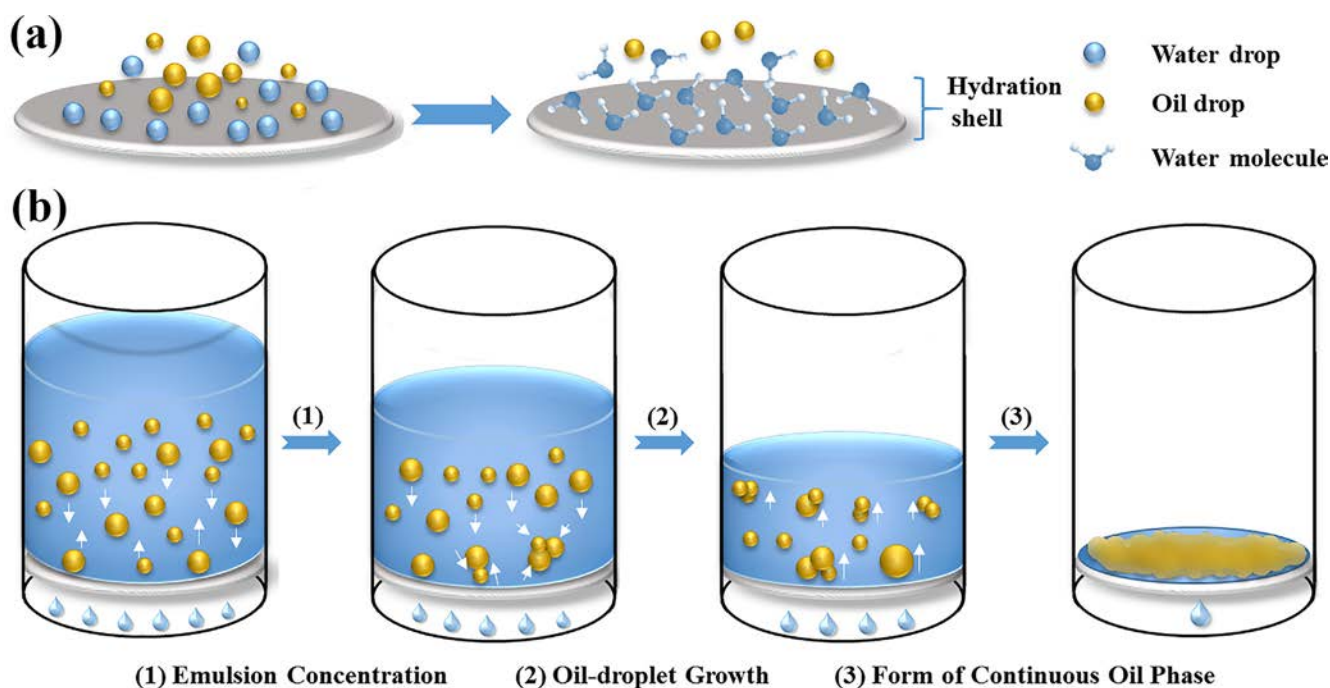


Fig. 12. Schematic diagram for the formation of (a) hydration shell and (b) possible mechanism of oil-in-water emulsion separation.

fouling performance among as-prepared membranes.

The CTAB and Tween 80 were also used as emulsifiers to prepare diesel-in-water emulsion to investigate the impact of different type of emulsifier on membrane performance. The filtrate flux of SDS-stabilized emulsion ( $721.2 \pm 29.7 \text{ L/m}^2\text{-h}$ ) was slightly higher than that of CTAB-stabilized one ( $689.2 \pm 25.4 \text{ L/m}^2\text{-h}$ ), while it was much lower of Tween 80-stabilized emulsion ( $415.1 \pm 16.2 \text{ L/m}^2\text{-h}$ ) (Fig. S12). The high filtrate flux of SDS and CTAB-stabilized emulsion might be related to the interaction between membrane surface and the charged surfactant. The electrostatic attraction or repulsion forces could assist the migration of surfactants on the surface of oil droplets when the charged droplets approached the membranes and consequently induced the demulsification of emulsions [40]. As for the obvious decrease in filtrate flux of Tween 80-stabilized emulsion, it might be explained by the high viscosity of the emulsion as shown in Table S1. In addition, the oil rejection towards different emulsions maintained at a high level as a result of the sieving effect.

The cyclic reusability and anti-fouling performance of M-TA5#3 were further evaluated. As exhibited in Fig. 11a, diesel-in-water emulsion flux stabilized at  $721.2 \pm 29.7 \text{ L/(m}^2\text{-h)}$  and the oil rejection kept at  $96.5\% \pm 0.5\%$  in 6 cycle tests. Besides diesel-in-water emulsion, Other four SDS-stabilized oil/water emulsions including n-hexane, kerosene, petroleum ether and dichloromethane were prepared and employed to test the performance of M-TA5#3. As shown in Fig. 11b–e, the stabilized emulsion flux of n-hexane-in-water, kerosene-in-water, petroleum ether-in-water and dichloromethane-in-water emulsions was  $670.3 \pm 24.2$ ,  $627.1 \pm 21.2$ ,  $664.3 \pm 24.6$  and  $1480.6 \pm 66.8 \text{ L/(m}^2\text{-h)}$ , respectively. Interestingly, the filtrate flux of dichloromethane-in-water emulsion was obviously higher than that of the other emulsions, which might be attributed to the larger oil droplets size compared to those of other emulsions [22]. The oil rejection towards different emulsions was  $96.5 \pm 0.5\%$ ,  $98.1\% \pm 0.5\%$ ,  $99.2\% \pm 0.3\%$ ,  $98.4\% \pm 0.4\%$  and  $97.2\% \pm 0.4\%$ , respectively, demonstrating the high separation efficiency of M-TA5#3. Fig. 11f showed that the FRR of the membrane was  $96.6\% \pm 0.3\%$ ,  $97.5\% \pm 0.4\%$ ,  $97.5\% \pm 0.4\%$ ,  $97.8\% \pm 0.3\%$  and  $97.7\% \pm 0.4\%$  for separating diesel, n-hexane, kerosene, petroleum ether and dichloromethane in water emulsions, respectively, after 6 cycle tests. Therefore, M-TA5#3 owned desirable

separation performance and decent reutilization property in separating different oil-in-water emulsions due to the facial superhydrophilic and underwater superoleophobic coating formed by TA and DEDAPS. For further improving the performance of membranes, the homemade PVDF membrane was prepared as substrate according to the previous work of our group [48]. After the co-deposition modification, the obtained membrane showed the extraordinary separation efficiency (all beyond 99.6%) and FRR (all above 98.5%) in separating various oil-in-water emulsions (Fig. S13). TA with intrinsic bio-adhesion offered the reaction sites for DEDAPS to bond, and the resulting co-deposition layer significantly enhanced the hydrophilicity of pristine PVDF membrane via introducing hydrophilic groups and the positive/negative charges.

Table 2 summarized a comparison of different membrane surface modification works in relative literatures for emulsion treatment. It can be seen that phenols were used to modify membranes with nano materials and macromolecules polymer, and all of them had achieved acceptable performance. In this work, the co-deposition of DEDAPS and TA constructed a superhydrophilic and underwater superoleophobic coating on membrane surface, conferring the membrane better performance compared with the membrane prepared in the listed literatures above. Hence, the co-deposition strategy endowed the membrane with competitive advantages of being employed to treat oil-in-water emulsions in practical process.

### 3.5. The plausible mechanism of modified PVDF membrane for emulsion separation

The co-deposition layer formed by TA and DEDAPS entitled the pristine PVDF membrane with superhydrophilicity and underwater superoleophobicity property. When the oil-in-water emulsion poured onto membrane surface, water molecules were prone to attach onto the surface of membrane, resulting in the formation of a stable and compact hydration shell (Fig. 12a). The formed hydration layer of the membrane surface could be used as a protective shield in preventing membrane from oil contacting and could produce an anti-intrusion pressure that blocked the permeation of oil [52]. As demonstrated in Fig. 12b, oil drop was repelled by hydration shell while the water penetrated through the membrane. With the decrease of water content, the oil

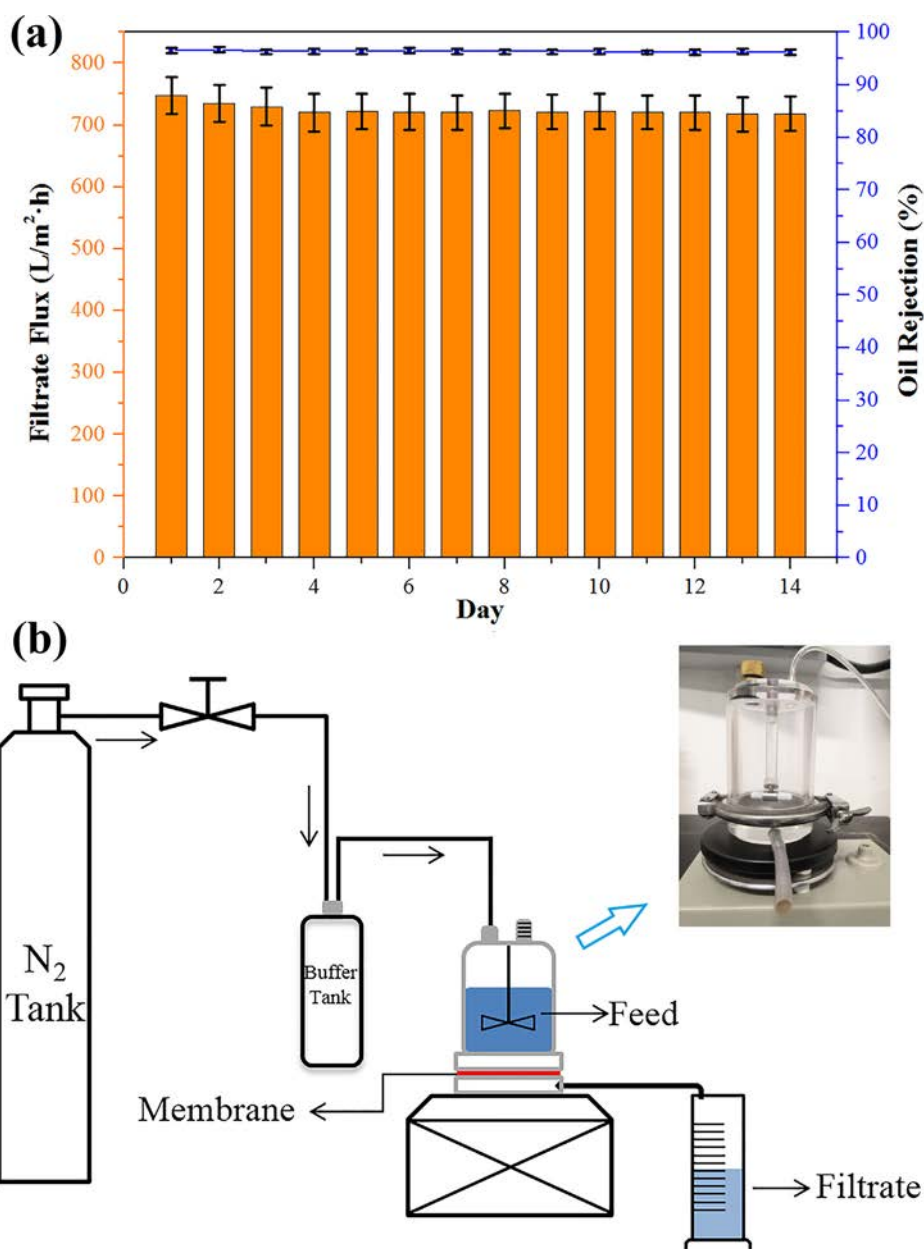


Fig. 13. (a) Filtrate flux and oil rejection of M-TA5#3 during long-term test and (b) diagram of device used for oil-in-water emulsion separation.

content began to increase. As a growing number of oil droplets aggregated on the interface, the size of oil droplet became expanded because of the coalescence effect [53]. Consequently, when the oil droplets grew up to enough size, they would depart from the ultralow adhesion membrane surface and then float up and finally form a continuous oil phase on account of Stokes law of resistance [54]. Thus, hydration shell protected the membrane from being fouled and facilitate the permeation of water in the process of separating oil-in-water emulsions.

### 3.6. Long-term stability of the optimized membrane

A long-term stability measurement was conducted to evaluate the sustainability of M-TA5#3. During 14-day test (Fig. 13a), the filtrate flux decreased from  $748.0 \pm 31.1$  to almost constant  $718.3 \pm 27.6$  L/(m<sup>2</sup>·h) within first 4 days and kept unchanged in following 10 days test, which was ascribed to that a small quantity of DADEPS on the surface of membranes fell off from membranes as experiments proceeding.

Though there was a little decrease in emulsion flux, the value still kept at a high level. Furthermore, the oil rejection was about  $96.2 \pm 0.5\%$  in the whole test. The diagram of separation device can be seen in Fig. 13b. In addition, there were almost no changes in the surface morphology and UOCA of modified membrane after long-term utilization (Fig. S14).

These results illustrated that the co-deposition layer constructed of DEDAPS and TA adhered to the surface of membranes tightly, which was due to the covalent bonding and non-covalent bindings including electrostatic attraction and hydrogen bond. In summary, M-TA5#3 maintained its desirable separation performance and surface anti-fouling property in long-term test, making it a decent candidate for treating oil-polluted emulsions in practical application.

## 4. Conclusions

In this work, a simple and efficient surface modification strategy, one-step co-deposition of TA and the newly synthesized micromolecular

zwitterionic substance (DEDAPS), was successfully employed to modify the hydrophobic PVDF membranes to improve its hydrophilicity and resistivity to oil-fouling. By varying the concentration of DEDAPS in co-deposition solution, the chemical constitution, surface morphology and PWF of the resultant membranes could be effectively adjusted. As is demonstrated by the experimental results, the optimal PVDF membrane showed superhydrophilicity and underwater superoleophobicity. The PWF of the optimized membrane could reach a value of  $4701.6 \pm 385.2 \text{ L}/(\text{m}^2\text{h})$ , which was 17 times that of pristine PVDF membrane. And it maintained high filtrate flux and oil rejection ( $> 96\%$ ) in treating various oil-in-water emulsions in the recycle tests and the long-term stability tests as a results of the robust hydrophilic coating formed by TA and DEDAPS. The super stability of co-deposition layer was further confirmed by the coating stability test. In summary, this study developed a durable and sustainable membrane for efficient oil-in-water emulsions separation, and provided an effective method for wastewater purification.

### Acknowledgments

We are grateful for the financial support from National Key R&D Program of China (No. 2016YFC0400406).

### Appendix A. Supplementary data

Supplementary data to this article can be found online at <https://doi.org/10.1016/j.seppur.2019.116015>.

### References

- [1] M.A. Shannon, P.W. Bohn, M. Elimelech, J.G. Georgiadis, B.J. Marinas, A.M. Mayes, Science and technology for water purification in the coming decades, *Nature* 452 (2008) 301–310.
- [2] I. Ali, New generation adsorbents for water treatment, *Chem. Rev.* 112 (2012) 5073–5091.
- [3] C. Liu, L. Wu, C. Zhang, W. Chen, S. Luo, Surface hydrophilic modification of PVDF membranes by trace amounts of tannin and polyethyleneimine, *Appl. Surf. Sci.* 457 (2018) 695–704.
- [4] G.D. Kang, Y.M. Cao, Application and modification of poly(vinylidene fluoride) (PVDF) membranes – a review, *J. Membr. Sci.* 463 (2014) 145–165.
- [5] X. Yang, H. Sun, A. Pal, Y. Bai, L. Shao, Biomimetic silicification on membrane surface for highly efficient treatments of both oil-in-water emulsion and protein wastewater, *ACS Appl. Mater. Interfaces* 10 (2018) 29982–29991.
- [6] Y. Lv, Y. Du, Z.X. Chen, W.Z. Qiu, Z.K. Xu, Nanocomposite membranes of poly-dopamine/electropositive nanoparticles/polyethyleneimine for nanofiltration, *J. Membr. Sci.* 545 (2018) 99–106.
- [7] N. Zhang, B. Jiang, L. Zhang, Z. Huang, Y. Sun, Y. Zong, H. Zhang, Low-pressure electroneutral loose nanofiltration membranes with polyphenol-inspired coatings for effective dye/divalent salt separation, *Chem. Eng. J.* 359 (2019) 1442–1452.
- [8] J. Albo, H. Hagiwara, H. Yanagishita, K. Ito, T. Tsuru, Structural characterization of thin-film polyamide reverse osmosis membranes, *Ind. Eng. Chem. Res.* 53 (2014) 1442–1451.
- [9] X. Wu, B. Zhao, L. Wang, Z. Zhang, J. Li, X. He, H. Zhang, X. Zhao, H. Wang, Superhydrophobic PVDF membrane induced by hydrophobic SiO<sub>2</sub> nanoparticles and its use for CO<sub>2</sub> absorption, *Sep. Purif. Technol.* 190 (2018) 108–116.
- [10] X. Mei, J. Liu, Z. Guo, P. Li, S. Bi, Y. Wang, Y. Yang, W. Shen, Y. Wang, Y. Xiao, X. Yang, B. Zhou, H. Liu, S. Wu, Simultaneous p-nitrophenol and nitrogen removal in PNP wastewater treatment: Comparison of two integrated membrane-aerated bioreactor systems, *J. Hazard. Mater.* 363 (2019) 99–108.
- [11] Z. Anari, A. Sengupta, K. Sardari, S.R. Wickramasinghe, Surface modification of PVDF membranes for treating produced waters by direct contact membrane distillation, *Sep. Purif. Technol.* 224 (2019) 388–396.
- [12] V. Vijayalakshmi, D. Khastgir, Chitosan/partially sulfonated poly(vinylidene fluoride) blends as polymer electrolyte membranes for direct methanol fuel cell applications, *Cellulose* 25 (2018) 661–681.
- [13] I. Banerjee, R.C. Pangule, R.S. Kane, Antifouling coatings: recent developments in the design of surfaces that prevent fouling by proteins, bacteria, and marine organisms, *Adv. Mater.* 23 (2011) 690–718.
- [14] Z.X. Wang, C.-H. Lau, N.Q. Zhang, Y.P. Bai, L. Shao, Mussel-inspired tailoring of membrane wettability for harsh water treatment, *J. Mater. Chem. A* 3 (2015) 2650–2657.
- [15] R. Zhang, Y. Liu, M. He, Y. Su, X. Zhao, M. Elimelech, Z. Jiang, Antifouling membranes for sustainable water purification: strategies and mechanisms, *Chem. Soc. Rev.* 45 (2016) 5888–5924.
- [16] G.V. Dizon, A. Venault, Direct in-situ modification of PVDF membranes with a zwitterionic copolymer to form bi-continuous and fouling resistant membranes, *J. Membr. Sci.* 550 (2018) 45–58.
- [17] P. Bengani-Lutz, E. Converse, P. Cebe, A. Asatekin, Self-assembling zwitterionic copolymers as membrane selective layers with excellent fouling resistance: effect of zwitterion chemistry, *ACS Appl. Mater. Interfaces* 9 (2017) 20859–20872.
- [18] A.C. Sagle, H. Ju, B.D. Freeman, M.M. Sharma, PEG-based hydrogel membrane coatings, *Polymer* 50 (2009) 756–766.
- [19] R. Reis, M. Duke, A. Merenda, B. Winther-Jensen, L. Puskar, M.J. Tobin, J.D. Orbell, L.F. Dumeé, Customizing the surface charge of thin-film composite membranes by surface plasma thin film polymerization, *J. Membr. Sci.* 537 (2017) 1–10.
- [20] O. Ojajuni, S. Holder, G. Cavalli, J. Lee, D.P. Saroj, Rejection of caffeine and carbamazepine by surface-coated PVDF hollow-fiber membrane system, *Ind. Eng. Chem. Res.* 55 (2016) 2417–2425.
- [21] Z. Wang, S. Ji, F. He, M. Cao, S. Peng, Y. Li, One-step transformation of highly hydrophobic membranes into superhydrophilic and underwater superoleophobic ones for high-efficiency separation of oil-in-water emulsions, *J. Mater. Chem. A* 6 (2018) 3391–3396.
- [22] W. Wu, R. Huang, W. Qi, R. Su, Z. He, Bioinspired peptide-coated superhydrophilic poly(vinylidene fluoride) membrane for oil/water emulsion separation, *Langmuir* 34 (2018) 6621–6627.
- [23] W. Zhang, Y. Zhu, X. Liu, D. Wang, J. Li, L. Jiang, J. Jin, Salt-induced fabrication of superhydrophilic and underwater superoleophobic PAA-g-PVDF membranes for effective separation of oil-in-water emulsions, *Angew. Chem., Int. Ed.* 53 (2014) 856–860.
- [24] Y. Zhu, J. Wang, F. Zhang, S. Gao, A. Wang, W. Fang, J. Jin, Zwitterionic nanohydrogel grafted PVDF membranes with comprehensive antifouling property and superior cycle stability for oil-in-water emulsion separation, *Adv. Funct. Mater.* 28 (2018) 1804121.
- [25] H. Lee, S.M. Dellatore, W.M. Miller, P.B. Messersmith, Mussel-inspired surface chemistry for multifunctional coatings, *Science* 318 (2007) 426–430.
- [26] Z. Wang, X. Jiang, X. Cheng, C.H. Lau, L. Shao, Mussel-inspired hybrid coatings that transform membrane hydrophobicity into high hydrophilicity and underwater superoleophobicity for oil-in-water emulsion separation, *ACS Appl. Mater. Interfaces* 7 (2015) 9534–9545.
- [27] T.S. Sileika, D.G. Barrett, R. Zhang, K.H.A. Lau, P.B. Messersmith, Colorless multifunctional coatings inspired by polyphenols found in tea, chocolate, and wine, *Angew. Chem., Int. Ed.* 52 (2013) 10766–10770.
- [28] D.G. Barrett, T.S. Sileika, P.B. Messersmith, Molecular diversity in phenolic and polyphenolic precursors of tannin-inspired nanocoatings, *Chem. Commun.* 50 (2014) 7265–7268.
- [29] H.A.M. Bacelo, S.C.R. Santos, C.M.S. Botelho, Tannin-based biosorbents for environmental applications – a review, *Chem. Eng. J.* 303 (2016) 575–587.
- [30] D. Ferreira, G.G. Gross, A.E. Hagerman, H. Kolodziej, T. Yoshida, Tannins and related polyphenols: perspectives on their chemistry, biology, ecological effects, and human health protection, *Phytochemistry* 69 (2008) 3006–3008.
- [31] Y.Z. Song, X. Kong, X. Yin, Y. Zhang, C.C. Sun, J.J. Yuan, B. Zhu, L.-P. Zhu, Tannin-inspired superhydrophilic and underwater superoleophobic polypropylene membrane for effective oil/water emulsions separation, *Colloids Surf. A* 522 (2017) 585–592.
- [32] Z. Wang, S. Ji, J. Zhang, F. He, Z. Xu, S. Peng, Y. Li, Dual functional membrane with multiple hierarchical structures (MHS) for simultaneous and high-efficiency removal of dye and nano-sized oil droplets in water under high flux, *J. Membr. Sci.* 564 (2018) 317–327.
- [33] M. He, K. Gao, L. Zhou, Z. Jiao, M. Wu, J. Cao, X. You, Z. Cai, Y. Su, Z. Jiang, Zwitterionic materials for antifouling membrane surface construction, *Acta Biomater.* 40 (2016) 142–152.
- [34] L.J. Zhu, F. Liu, X.M. Yu, A.L. Gao, L.X. Xue, Surface zwitterionization of hemocompatible poly(lactic acid) membranes for hemodiafiltration, *J. Membr. Sci.* 475 (2015) 469–479.
- [35] T. Ma, Y. Su, Y. Li, R. Zhang, Y. Liu, M. He, Y. Li, N. Dong, H. Wu, Z. Jiang, Fabrication of electro-neutral nanofiltration membranes at neutral pH with antifouling surface via interfacial polymerization from a novel zwitterionic amine monomer, *J. Membr. Sci.* 503 (2016) 101–109.
- [36] P. Kaner, E. Rubakh, D.H. Kim, A. Asatekin, Zwitterion-containing polymer additives for fouling resistant ultrafiltration membranes, *J. Membr. Sci.* 533 (2017) 141–159.
- [37] A. Venault, H.S. Yang, Y.C. Chiang, B.S. Lee, R.C. Ruaan, Y. Chang, Bacterial resistance control on mineral surfaces of hydroxyapatite and human teeth via surface charge-driven antifouling coatings, *ACS Appl. Mater. Interfaces* 6 (2014) 3201–3210.
- [38] M.A. Rahim, H. Ejima, K.L. Cho, K. Kempe, M. Muellner, J.P. Best, F. Caruso, Coordination-driven multistep assembly of metal-polyphenol films and capsules, *Chem. Mater.* 26 (2014) 1645–1653.
- [39] C. Wei, F. Dai, L. Lin, Z. An, Y. He, X. Chen, L. Chen, Y. Zhao, Simplified and robust adhesive-free superhydrophobic SiO<sub>2</sub>-decorated PVDF membranes for efficient oil/water separation, *J. Membr. Sci.* 555 (2018) 220–228.
- [40] J. Wu, W. Wei, S. Li, Q. Zhong, F. Liu, J. Zheng, J. Wang, The effect of membrane surface charges on demulsification and fouling resistance during emulsion separation, *J. Membr. Sci.* 563 (2018) 126–133.
- [41] R. Zhou, P.F. Ren, H.-C. Yang, Z.K. Xu, Fabrication of antifouling membrane surface by poly(sulfobetaine methacrylate)/polydopamine co-deposition, *J. Membr. Sci.* 466 (2014) 18–25.
- [42] J. Guo, Y. Ping, H. Ejima, K. Alt, M. Meissner, J.J. Richardson, Y. Yan, K. Peter, D. von Elverfeldt, C.E. Hagemeyer, F. Caruso, Engineering multifunctional capsules through the assembly of metal-phenolic networks, *Angew. Chem., Int. Ed.* 53 (2014) 5546–5551.
- [43] S. Zhang, Z. Jiang, X. Wang, C. Yang, J. Shi, Facile method to prepare microcapsules

- inspired by polyphenol chemistry for efficient enzyme immobilization, *ACS Appl. Mater. Interfaces* 7 (2015) 19570–19578.
- [44] Y.F. Mi, F.Y. Zhao, Y.S. Guo, X.D. Weng, C.-C. Ye, Q.-F. An, Constructing zwitterionic surface of nanofiltration membrane for high flux and antifouling performance, *J. Membr. Sci.* 541 (2017) 29–38.
- [45] J. Drelich, E. Chibowski, Superhydrophilic and superwetting surfaces: definition and mechanisms of control, *Langmuir* 26 (2010) 18621–18623.
- [46] N.J. Shirtcliffe, G. McHale, S. Atherton, M.I. Newton, An introduction to superhydrophobicity, *Adv. Colloid Interface Sci.* 161 (2010) 124–138.
- [47] S. Wang, K. Liu, X. Yao, L. Jiang, Bioinspired surfaces with superwettability: new insight on theory, design, and applications, *Chem. Rev.* 115 (2015) 8230–8293.
- [48] L. Zhang, Z. Shu, N. Yang, B. Wang, H. Dou, N. Zhang, Improvement in antifouling and separation performance of PVDF hybrid membrane by incorporation of room-temperature ionic liquids grafted halloysite nanotubes for oil-water separation, *J. Appl. Polym. Sci.* 135 (2018).
- [49] B.D. McCloskey, H.B. Park, H. Ju, B.W. Rowe, D.J. Miller, B.D. Freeman, A bioinspired fouling-resistant surface modification for water purification membranes, *J. Membr. Sci.* 413 (2012) 82–90.
- [50] Z. Liu, W. Wu, Y. Liu, C. Qin, M. Meng, Y. Jiang, J. Qiu, J. Peng, A mussel inspired highly stable graphene oxide membrane for efficient oil-in-water emulsions separation, *Sep. Purif. Technol.* 199 (2018) 37–46.
- [51] X. Ruan, Y. Xu, X. Liao, G. He, X. Yan, Y. Dai, N. Zhang, L. Du, Polyethyleneimine-grafted membranes for simultaneously adsorbing heavy metal ions and rejecting suspended particles in wastewater, *AIChE J.* 63 (2017) 4541–4548.
- [52] J. Ge, J. Zhang, F. Wang, Z. Li, J. Yu, B. Ding, Superhydrophilic and underwater superoleophobic nanofibrous membrane with hierarchical structured skin for effective oil-in-water emulsion separation, *J. Mater. Chem. A* 5 (2017) 497–502.
- [53] S. Gao, J. Sun, P. Liu, F. Zhang, W. Zhang, S. Yuan, J. Li, J. Jin, A robust polyionized hydrogel with an unprecedented underwater anti-crude-oil-adhesion property, *Adv. Mater.* 28 (2016) 5307–5314.
- [54] J.S. Lintuvuori, K. Stratford, M.E. Cates, D. Marenduzzo, Colloids in cholesterics: size-dependent defects and non-stokesian microrheology, *Phys. Rev. Lett.* 105 (2010) 178302.